

On-line 3-D reconstruction of cardiac chambers via topographic cellular algorithms from echocardiographic sequences

D. Hillier*, Zs. Czeilinger\$ and Cs. Rekeczky*+

+Analogical and Neural Computing Systems Laboratory
Computer and Automation Research Institute

Hungarian Academy of Sciences, Budapest, Hungary

*Jedlik Laboratories, Department of Information Technology,
Péter Pázmány Catholic University, Budapest, Hungary

\$Pediatric Heart Center, Hungarian Institute of Cardiology

Email: hillier@digitus.itk.ppke.hu

Abstract– A new method for 3D reconstruction and quantitative analysis of cardiac cavities based on topographic cellular active contour (TCAC) techniques was developed aiming on-line visualization of cardiac chambers. TCAC algorithms perform boundary contour tracking in video real-time speed on 2D projections taken at different angles by an electronically controlled transducer. The 3D view of the human heart is reconstructed from these contours. The whole process was implemented on the ACE-BOX platform exploiting the power of CNN processors.

Performance of TCAC methods was assessed by comparison with manually traced echocardiographic video flows by independent cardiologist experts. For the selected clinical examples, error of our algorithms proved to be comparable to the inter-observer variability between independent experts. Validation of accuracy of volume quantification was performed on 60 in-vitro static objects. The clinical potential of our system is demonstrated by 3D reconstruction of two cardiac chambers with interactive planning of surgical interventions.

1. Introduction

Ultrasound techniques allow direct visualization of the heart in motion. Diagnostic algorithm concepts in echocardiography changed abruptly in the last decade. It is now widely recognized that quantitative analysis of echocardiograms is preferable over qualitative interpretation, in particular for wall motion and volume estimation. However, manual measurements are time consuming and suffer from considerable inter- and intraobserver variability.

Many effort has been done to develop 3D quantitative volumetric imaging methods to tackle these problems. Active contour (AC) based methods became quite popular for cardiac boundary detection that is an essential step before 3D reconstruction and quantitative analysis. However, most AC techniques are computationally intensive that limits their application in tasks requiring fast response, like real time echocardiography. Compared to existing AC techniques (see e.g. [2]) our approaches resolve the high computational cost by discretizing the contours and performing parallel computational operations

on each contour pixel thus keeping the efficiency of active contour techniques with uncompromised detection speed.

Accuracy of boundary detection and of 3D reconstruction is a key toward clinical introduction of a method. To our best knowledge, applicability of all published approaches is limited to the left ventricle (LV) of the human heart. A major contribution of our work is that our on-line 3D reconstruction environment based on TCAC methods is not restricted to the LV.

In the sequel we shall first briefly introduce and compare three different TCAC methods, all implemented on a common platform and tested within the same environment. Then we present results from in-vitro validation of the system and finally 3D reconstruction of a selected clinical example will be shown.

2. Boundary tracking: Theory

The task of TCAC algorithms is to detect a coherent boundary in between the dark and light image regions, i.e. we have to find the boundary between dark ventricles surrounded by brighter cardiac walls in a grayscale echocardiography video flow. In our framework an active contour evolves from its initial shape and position under the influence of external and/or internal driving forces. The external forces attract the contour to image features to be detected whereas internal forces can model the elasticity of the curve and balance the influence of external forces. The evolution of discrete curve points can be implemented either by iterative or by dynamic methods. The main difficulties to be overcome reside in the initialization of the contour tracking and the handling of

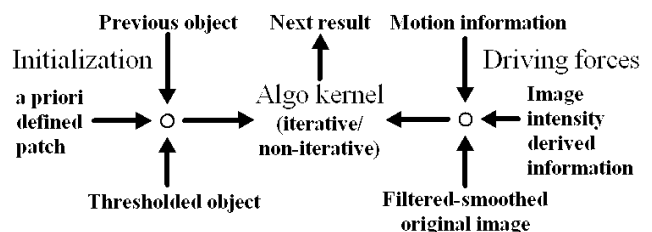


Figure 1. The algorithm kernel computes the evolution of curve pixels under the influence of internal and external driving forces. The initial contour can be obtained by either defining it a priori or by extracting an initial feature map obtained from the input image

false or missing features on the input image. Once the contour has been initialized the quality and speed of subsequent contour detections can be substantially improved by exploiting the correlation between consecutive frames. Topographic active contour techniques make use of the result from the previous iteration which is used to initialize the current contour detection.

3. Boundary tracking: Implementations

In the initial stage – in all of our algorithms – preprocessing is needed to eliminate speckle noise from the input images. Input data is a discretized, grayscale image taken from an ultrasound (US) video flow (or “3D data cube”) at a specific time instance. For the first frame, a calibrating module provides the algorithms with initial parameters adapted to the input image under processing. It cuts out 1D samples from the image in radial directions, and uses a Sobel-like 1D edge detection operator on each to find the point where the sampling line intersects the cardiac contour. It outputs the approximate position and size of the target object with the average illumination level of the cardiac chamber and wall. We shall now give a brief overview of our TCAC algorithms. For an in-depth description, see [3] and references therein.

3.1. Constrained Wave Computing

In Constrained Wave Computing the contour to be detected is the steady contour of a dynamic wave initiated from patches called sources. The evolution of the dynamic wave can be stopped using a grayscale spatial constraint calculated from the input image(s). Where wall segments are missing on the US image, proper spatial constraint or external force cannot be generated to stop the wave propagation. However, a properly chosen time-constraint can always be applied and thus a solution will be obtained in a non-equilibrium state of the network. In summary, in the case of CWC the task to be solved should be converted into adequate spatio-temporal constraints.

3.2. Pixel Level Snakes

In contrast to CWC, the Pixel Level Snakes method solves the contour tracking task in an iterative fashion using topographic cellular operations.

The contour evolution is based on binary and local morphological operations which perform a directional contour expansion of the active contour followed by a directional contour thinning along the four cardinal directions. These operations are driven by guiding information extracted from the image being processed as external forces and from the contour itself as internal and balloon forces.

The external potential is derived from the input image features to establish a map of external forces. The contour will evolve in those directions where the potential field decreases. This external potential should be defined in such a way that its valleys coincide with the boundaries of the region of interest. This step is strongly dependent on the particular application PLS is used to solve and

therefore represents an external input to the algorithm.

The internal potential is derived directly from the active contour itself. It represents a curvature dependent control over the evolution of the active contour to ensure its appropriate, application dependent smoothness level. In the guiding force extraction (GFE) module, a directional gradient operation on the resulting image will then originate positive internal forces that will reduce local curvature or – in other words – smooth the contour shape. Due to the inherent nature of curvature driven internal forces the contour has a shrinking tendency. To counteract this issue along with the necessity to trespass spurious isolated weak image edges an additional inflating force field called balloon force is introduced.

In the end, by summing the weighted external, internal and inflating potentials we obtain the global potential field on which a directional gradient operation is performed to serve the GFE module. In a pixel-level iterative technique only the sign of the guiding forces along the direction under exploration is actually needed. The GFE module creates a binary map with activated pixels in those locations where the potential is decreasing along the direction under study. Thus the contour evolution is allowed where this map contains activated pixels.

3.3. Moving Patch Method

This topographic active contour algorithm works on a “patch image”, which initially contains a black patch acquired from the system-level calibration module. It also uses a “control image”, which might contain the raw echocardiographic video frame itself, or an image preprocessed with the MaxShadow algorithm (see [3] for details).

This algorithm is iterative like the PLS, but it differs from PLS in that it uses a filled black-and-white patch to represent the contour, so the inner and outer side of the contour is unambiguous even if we look at only the local neighborhood of the contour pixels. The patch image will be modified in each iteration under the guidance of local rules operating on 3x3 neighborhoods of the patch and control image, until the patch fits the endocardial boundary.

The contour evolution has two kinds of constraints: the internal constraints are related only to the patch image, responsible for the well-formedness of the patch; and the external constraints, which use the features of the control image. In each iteration, many decisions are made for each pixel of the patch image, and the result of these decisions is the new value of that pixel.

The internal constraints have the form of HitAndMiss masks. First the “must be black” masks are checked: these masks set those pixels of the patch image black, which have a neighborhood of more than four black pixels. This rule ensures that the patch will not contain singular white pixels, and also fills up the deeper concavities of the contour. Since cardiac chambers are mostly convex, the surface tension imposed by this rule smooths out small errors of the contour.

Next the “valid black” masks are checked: these select those pixels, which have exactly three neighboring black pixels, and these pixels are adjacent to each other. Only these pixels are subject to the external constraint checking: these are the pixels where the contour can expand or shrink. All other pixels, selected neither by the “must be black”, nor the “valid black” masks are turned to white: this eliminates singular black pixels disconnected from the main patch.

Pixels where the contour is allowed to expand or shrink will be checked against global threshold values. The pixels of the control image where the patch image is allowed to move, are checked whether they fall below or above a lower and higher global threshold level, and they are turned black or white, respectively. These thresholds are responsible for the unconditional expansion or shrinking of the contour in regions belonging unequivocally to chambers or myocardium.

For the remaining pixels, the algorithm calculates the average grayscale level of the neighboring pixels on the control image corresponding to the “black” and “white” pixels in the patch image, respectively. If the difference between these “white” and “black” average values is below a local difference threshold, it turns the pixel white, otherwise to black.

This last step is the essential contour detection step. By computing the intensity difference between the inner and outer side of the contour, the algorithm approximates the component of the local gradient which is orthogonal to the contour. The contour is expanding if the intensity gradient is greater than a local difference threshold, and shrinking when it is less. In other words, if we approach the cardiac wall from inside the cardiac chamber, we will see a gradual increase in the average intensity, until we reach the intensity plateau of the cardiac wall. This change of gradient amplitude is detected by this approach.

4. Boundary tracking using TCAC methods: Comparison

Table 1 shows major theoretical and implementational aspects of our TCAC algorithms. Note that a priori motion information between current and previous and eventually the between the next frame is only exploited in CWC. This information could be important in several cases when false edges appear in the frame sequence. PLS differs from the other methods representing the active contour explicitly compared to CWC and MPM which detect contours in each iteration starting from a kernel.

PLS and MPM have an inherent capability to deflate the contour or let parts of the contour move inwards. In contrast, CWC is an expansive method but it can handle inward moving contour segments by shrinking the previous result to obtain the kernel for the current frame.

When speaking about performance and quality issues, we have to keep in mind that it is extremely difficult to quantitatively compare two different active contour algorithms. We went as far as possible in implementing the three algorithms in a common framework. Current analogic architectures (we have worked mainly on the

ACE4k chip [4] and also on the ACE16k chip [5] embedded within the ACE-BOX environment) provide a fixed complexity reproducible CNN computing (nearest neighbor computing with linear CNN templates). The PLS core is using linear uncoupled CNN templates and shows impressing detection speed (25 fps) and accuracy running on the ACE4k chip. The full version of MPM is currently implemented using non-linear uncoupled operations running on the DSP platform of the ACE-BOX architecture. MPM is the most robust method at the expense of currently running only at 22 fps with non-topographic optimizations. Note that PLS is a general technique whereas MPM with MaxShadow implements various echocardiography-specific heuristics. CWC is a dynamic method using linear coupled CNN templates. CWC was implemented on the ACE16k platform and uses only 1.3 ms per frame for all the template operations.

	<i>CWC</i>	<i>PLS</i>	<i>MPM</i>
Information exchange in space	acausal cellular nearest neighbor	acausal cellular nearest neighbor	acausal cellular nearest neighbor
Information exchange in time	acausal recursive nearest frame	causal recursive nearest frame	causal recursive nearest frame
Contour representation	implicit, region prop.	explicit, curve prop.	implicit, region prop.
Contour localization technique	expansive	expansive / contractive	expansive / contractive
Computation method	PDE related	“energy” related	rule based
Implementation	Dynamic	Iterative	Iterative
Minimal complexity of CNN formulation	Linear coupled	Linear coupled	Non-linear uncoupled
ACE-BOX implementation	Complete, Ace16k	Complete, Ace4k	Complete, DSP

Table 1 Major theoretical and implementational aspects of our TCAC algorithms

4.1. Quality assessment of TCAC methods

In order to validate the quality of TCAC algorithms we used a database containing more than 1000 video flows of clinical data from which around 600 flows have reference, manually traced by cardiologist experts. For 6 video-flows, four independent experts have manually traced the endocardial boundary. In those cases where four references were available we calculated a common mean or “golden-standard” reference using a topographic approach, described in detail in [3].

5. 3D reconstruction

Analysis of 2D slices (filtering, segmentation, contour tracking and content/context based recognition) was designed as a set of analogic CNN-UM algorithms. Contours are adaptively resampled, then rotated and translated into the 3D space on the DSP.

From this dataset, the 3D reconstruction module first produces a polygon based model in real-time that allows a dynamic feedback to contour tracking in order to adaptively correct the errors introduced in that phase. Then the on-line renderer engine computes the final 3D model (see Figure 2) using metaball algorithm [6] when data for all chambers of interest have been processed by the boundary tracking module. 3D diagnostic information e.g. cavity volumes are obtained directly from the 3D geometrical model.

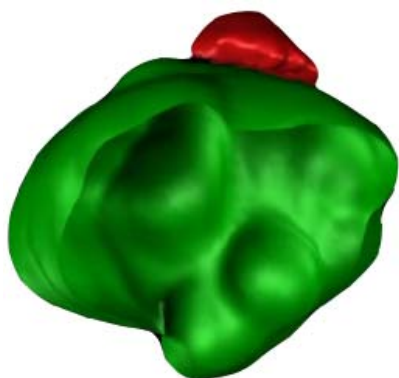


Figure 2. 3D reconstruction of two atria of a human heart

6. Validation

We validated the accuracy of our on-line 3D echocardiography system using static in vitro dummy objects. 60 rubber balloons with diverse geometry, simulating a heart cavity have been filled with water, sealed and placed in water bath (60, 100 and 250 ml, 20 pieces of each volume). The inner boundary detection of each object was performed using PLS algorithm. Statistics of reconstructed volumes can be seen on Table 2.

Volume of phantoms (ml)	60.00	100.00	120.00
Mean of 20 samples	59.26	101.56	248.04
Standard dev. of samples	2.82	4.21	4.93

Table 2 Result of validation measurements

7. Discussion and conclusions

The major result of this study is to bring real-time TCAC based on-line 3D reconstruction system into clinical test phase.

When comparing results of boundary detection methods to the inter-observer variability between hand-traced contours produced by different cardiologist experts, one can hardly draw a clear conclusion. For some selected examples, error between the output of our TCAC algorithms and the expert-traced reference is in average around 10%. For the selected examples this is a good

achievement since it is very slightly higher than the error between two references traced by two independent experts.

Since all curves are similar it is important to keep in mind that balancing speed requirement for real-time echocardiography with keeping hardware complexity at an affordable level to allow future industrial production cannot be done without relaxing our expectations towards the exact fitting of our results to expert traced contours. The novel visualisation technique of our system includes geometry independent quantitative measurements of the heart cavities. Currently available quantitative imaging methods are either more invasive and involve radiation exposure such as angiography, CT and MRI or they cannot be properly applied to assymmetric cavities such as atria or the right ventricle. Each available method having different degree of reliability and currently there is no obligatory gold standard for the volumetry of assymmetric heart cavities [7].

Acknowledgments

Thanks are due to the entire research and development team at ANCL and AnaLogic-Computers Ltd. for the ongoing work related to the ACE-BOX system and computational infrastructures (Aladdin Pro 3.x software system [8]).

The authors also would like to acknowledge the support for this research through the Hungarian National Research and Development Program, "TeleSense" (NKFP 035/02/2001).

References

- [1] T. Roska and L. O. Chua, "The CNN Universal Machine", IEEE Trans. on Circ. & Syst., Vol. 40, pp. 163-173, 1993.
- [2] V. Chalana et al., "A Multiple Active Contour Model for Cardiac Boundary Detection on Echocardiographic Sequences", IEEE TMI, Vol.15, No. 3, pp. 290-298, 1996.
- [3] D. Hillier et al., "Topographic Cellular Active Contour Techniques: Theory, Implementations and Comparisons", Intl. Journal of Circ. Theory and Appl., accepted for publication, 2005.
- [4] S. Espejo et al., "A 64 64 CNN Universal Chip with Analog and Digital I/O", in Proc. ICECS'98, pp. 203-206, Lisbon 1998.
- [5] A. Rodriguez-Vazquez et al., "ACE16k: The Third Generation of Mixed-Signal SIMD-CNN ACE Chips Toward VSoCs", IEEE Trans. on Circuits and Systems—I, Vol. 51, No. 5, May 2004
- [6] H. Nishimura et al., "Object Modeling by Distribution Function and a Method of Image Generation", Trans. on IECE 68-D(4): 718725, 1985
- [7] S. Kovalova et al., "Echocardiographic volumetry of the right ventricle", Eur. Jour. of Echocard, vol 6; 1: 15-23, 2005
- [8] Analogic Computers Ltd: Aladdin Pro V3.x. <http://www.analogic-computers.com>, Budapest, 2004.